European Journal of Taxonomy 753: 1–80
https://doi.org/10.5852/ejt.2021.753.1389
ISSN 2118-9773
www.europeanjournaloftaxonomy.eu
2021 · Tissier J. *et al.*

Monograph

urn:lsid:zoobank.org:pub:8009DD3B-53B0-45C9-921E-58D04C9C0B48

New species, revision, and phylogeny of *Ronzotherium* Aymard, 1854 (Perissodactyla, Rhinocerotidae)

Jérémy TISSIER[1,*], Pierre-Olivier ANTOINE[2] & Damien BECKER[3]

[1,3]Route de Fontenais 21, JURASSICA Museum, 2900 Porrentruy, Switzerland & Chemin du musée 4, Université de Fribourg, Department of Geosciences, 1700 Fribourg, Switzerland.
[2]Place Eugène Bataillon, Institut des sciences de l'évolution de Montpellier-CNRS-IRD-RPHE, Université de Montpellier, 34095 Montpellier, France.

[*]Corresponding author: jeremy.tissier123@gmail.com
[2]Email: pierre-olivier.antoine@umontpellier.fr
[3]Email: damien.becker@jurassica.ch

[1]urn:lsid:zoobank.org:author:7418361D-FAA0-4D7D-AE4A-80B5C9288B31
[2]urn:lsid:zoobank.org:author:61FBD377-963B-4530-A4BC-0AB4CBCAD967
[3]urn:lsid:zoobank.org:author:E1D8E6B2-6F92-4B0B-A772-4F5C561851DB

Abstract. *Ronzotherium* is one of the earliest Rhinocerotidae in Europe, which first appeared just after the Eocene/Oligocene transition (Grande Coupure), and became extinct at the end of the Oligocene. It is a large-sized rhinocerotid, with a special position in the phylogeny of this group, as being one of the earliest-branching true Rhinocerotidae. However, its intra-generic systematics has never been tested through computational phylogenetic methods and it is basically unknown. Its taxonomical history has gone through numerous complications, and thus we aim to provide here a complete revision of this genus, through phylogenetic methods. After a re-examination of all type specimens (five supposed species) as well as of most well-preserved specimens from all over Europe and ranging through the complete Oligocene epoch, we performed a parsimony analysis to test the position of some problematic specimens. According to our results, five species can be distinguished, *Ronzotherium velaunum* (type species), *R. filholi*, *R. elongatum* and *R. romani* as well as a new species: *R. heissigi* sp. nov. We also drastically re-interpret its anatomy and show that the 'short-limbed' "*Diaceratherium*" *massiliae*, described from Southern France, can be considered as a junior synonym of *R. romani*. Finally, we exclude the Asian species "*Ronzotherium*" *orientale* and "*Ronzotherium*" *brevirostre* from *Ronzotherium* and we consider *R. kochi* as a junior synonym of *R. filholi*.

Keywords. Europe, taxonomy, Oligocene, Grande Coupure, phylogeny.

Tissier J., Antoine P.O. & Becker D. 2021. New species, revision, and phylogeny of *Ronzotherium* Aymard, 1854 (Perissodactyla, Rhinocerotidae). *European Journal of Taxonomy* 753: 1–80.
https://doi.org/10.5852/ejt.2021.753.1389

Introduction

The genus *Ronzotherium* Aymard, 1854 is the most typical rhinocerotoid in the Oligocene of Europe. It was a hornless, medium- to large-sized rhinoceros, that notably appeared during the Grande Coupure

event, and survived until the latest Oligocene (Heissig 1969; Brunet 1979). The Grande Coupure event, first termed by Stehlin (1909), refers to an extinction and possibly migration-related event, occurring just after the Eocene/Oligocene boundary in Western Europe. *Ronzotherium* is one of the markers of this event, as one of the earliest European rhinocerotids, along with *Epiaceratherium* Abel, 1910 (Brunet 1979; Uhlig 1999a, 1999b; Becker 2009). It is also of particular interest for the evolution of the Rhinocerotidae because of its systematic position as one of the earliest-branching rhinocerotids (e.g., Cerdeño 1995), and shows some relatively primitive characters compared with more derived rhinocerotids such as the presence of two well-developed upper incisors, and very poorly molarised premolars (Brunet 1979).

Regrettably, the taxonomical history of this genus is quite confused, and it remains a poorly studied taxon, despite its phylogenetic and biogeographical significance. The genus *Ronzotherium* was first named after the hill of Ronzon by the French paleontologist Aymard in 1854, from material found in his hometown of Le Puy-en-Velay, which gave its name to *R. velaunum* (Aymard in Pictet, 1853). This locality of Ronzon is significant for the study of Western European Oligocene faunas because it has been dated from MP21 (earliest Oligocene) and is very rich, preserving numerous vertebrate and invertebrate taxa. Yet, it was Filhol (1881) who first illustrated and described most of the mammalian taxa from Ronzon, including *R. velaunum*, almost 30 years after its first mention. This probably explains why no new material was attributed to this genus until Osborn (1900) wrongly referred a lower jaw from Brons (Cantal, France) to *Ronzotherium gaudryi* Osborn, 1900. This species is now attributed to the genus *Eggysodon* Roman, 1910 (Rhinocerotoidea, Eggysodontidae Breuning, 1923), like several others that have also been erroneously attributed to *Ronzotherium* such as *Eggysodon osborni* (Schlosser, 1902) or *Eggysodon reichenaui* (Deninger, 1903), notably because of the presence of upper and lower canines. Because of these complications and the absence of explicit definition of *Ronzotherium* by Aymard (1854), Roman (1912a) advocated that the name "*Ronzotherium*" should be forgotten and replaced by *Aceratherium*, but the name nonetheless persisted.

By complete chance, Osborn (1900) also named in the same publication a new species *Acerotherium filholi* Osborn, 1900 based on material from the Phosphorites du Quercy, it now indeed belongs to *Ronzotherium*. Later, this species was also discovered in several localities of Switzerland (Stehlin 1903; Jenny 1905) and France (Roman 1912a), although it was also confused with *Diaceratherium* (e.g., Roman 1912a: pl. V figs 4–5, even though Roman admitted his doubts on this attribution).

Almost thirty years after the work of Roman (1912a), the Hungarian palaeontologist Miklós Kretzoi dedicated him a new species, *Ronzotherium romani* Kretzoi, 1940, based on his illustration of a lower incisor from La Ferté-Alais (Roman 1912a: fig. 17). Even though this species was only named in a footnote of the paper (Kretzoi 1940), without either a proper diagnosis or direct observation, the species remained valid and was accepted by subsequent authors. In particular, several specimens were attributed to this taxon by Heissig (1969), after an almost exhaustive revision of this genus.

In that work, Heissig considered *R. romani* as a subspecies of *R. filholi*, along with a new subspecies, *Ronzotherium filholi elongatum* Heissig, 1969. This large-scale work brought a significant clarification of the genus *Ronzotherium* by identifying numerous specimens and delivered the first and only (handmade) phylogenetic representation of this genus. Yet, this revision remained incomplete, since only dental and mandibular remains were considered. Ten years later, Brunet (1979) also conducted a large-scale revision of this genus in his PhD thesis, focusing on the material from Villebramar (France), which delivered numerous specimens of *R. filholi*, including one well-preserved skull (the third only known for this genus to have ever been described). Based on his observations, he refuted the existence of *R. elongatum* that he considered a junior synonym of *R. filholi* and he reconsidered *R. romani* as a species. Contrary to Heissig (1969), Brunet (1979) considered the evolution of *Ronzotherium* as fully

anagenetic: *R. velaunum* evolved into *R. filholi*, which evolved into *R. romani*. However, this hypothesis is not based on any phylogenetic evidence, and is only supported by stratigraphy, following a then-popular model of phyletic gradualism.

Finally, even though *Ronzotherium* is mostly a Western European taxon, several non-Western European species have been attributed to this genus, notably *Ronzotherium kochi* Kretzoi, 1940 from Romania or *Ronzotherium brevirostre* (Beliayeva, 1954) from Mongolia (Dashzeveg 1991; = "*R.*" *orientale* according to Antoine *et al*. 2003). However, they have only been partly revised, and remain very poorly known.

Thus, we propose here a quasi-exhaustive revision of this genus, aiming at elucidating its systematics by using methods of computational phylogenetics, at the population level. Using populations (i.e., ronzothere remains from a single locality) helps understanding the evolutionary history of the genus by taking into consideration the type morphology, as well as the intraspecific variability. After considering this variability, we tested the position of this genus within a larger-scale phylogeny.

Our results, based on direct observation of every type and most major localities of *Ronzotherium* permit us to re-identify several specimens, and they support the validity of five Western European species: the type species *Ronzotherium velaunum* (Aymard in Pictet, 1853), *Ronzotherium filholi* (Osborn, 1900), *Ronzotherium romani* Kretzoi, 1940, *Ronzotherium elongatum* Heissig, 1969 and *Ronzotherium heissigi* sp. nov. Based on the phylogenetic results, each species can now be properly diagnosed and described. This complete revision allows us to discuss the evolution of *Ronzotherium* altogether, and we suggest that cingulum may have played a central role in the persistence of *R. romani* until the end of the Oligocene epoch. We also tentatively investigate the relation between age, geography, and body mass, and suggest that there is no correlation between the evolution of the body mass and these parameters.

Material and methods

Institutional abbreviations

The specimens discussed in this study are deposited in the following institutions:

AIX = Muséum d'histoire naturelle d'Aix-en-Provence (France)
BSPG = Bayerische Staatssammlung für Paläontologie und Geologie, Munich (Germany)
FSL = Collections de la Faculté des Sciences de Lyon (France)
MBT = Muzeul de Paleontologie-Stratigrafie, Universitatea Babeş-Bolyai, Cluj-Napoca (Romania)
MGL = Musée cantonal de géologie de Lausanne (Switzerland)
MHNB41 = Muséum d'histoire naturelle de Blois (France)
MHNM = Muséum d'histoire naturelle de Marseille (France)
MNHN = Muséum national d'histoire naturelle, Paris (France)
MJSN = Jurassica Museum of Porrentruy (Switzerland)
NMB = Naturhistorisches Museum Basel (Switzerland)
NMBE = Naturhistorisches Museum der Burgergemeinde Bern (Switzerland)
NMO = Naturmuseum Olten (Switzerland)
SMNS = Staatliches Museum für Naturkunde Stuttgart (Germany)
PUY = Musée Crozatier, Le Puy-en-Velay (France)
TLM = Muséum d'histoire naturelle de Toulouse (France)
UM = Université de Montpellier (France)

Surface scanning

Numerous specimens were scanned with a structured-light surface scanner (Artec Space Spider, Artec Group) and the 3D models have been reconstructed using the Artec Studio 13 Professional software.

Some of these 3D models are presented in the figures of this study, with texture (e.g., Fig. 3A), or without (e.g., Fig. 3B–D). In most cases, representing 3D models without the texture enhances the contrast and shadows to distinguish articulation surfaces.

Anatomy and anatomical abbreviations

The characters described follow the terminology of Antoine (2002). The estimation of the body mass follows the equations for Rhinocerotidae of Fortelius & Kappelman (1993: appendix 1) based on cranial, dental, humeral, radial, femoral and tibial measurements, as well as the best predictors for the equation of Tsubamoto (2014) based on astragalar measurements: Li1, Ar1 and Ar3.

Dental abbreviations

Cc = calcaneus
d/D = lower/upper decidual tooth
i/I = lower/upper incisor
m/M = lower/upper molar
Mc = metacarpal
Mt = metatarsal
p/P = lower/upper premolar

Dental measurements are provided in Supp. file 1, and postcranial measurements are provided in Supp. file 2, for all species of *Ronzotherium*.

Phylogeny

The taxonomical sampling includes all the specimens from the type localities of Ronzon for *Ronzotherium velaunum* and La Ferté-Alais for *R. romani* as well as the holotype and 'cotype' of *R. filholi* designated by Osborn (1900) from the Phosphorites du Quercy, the holotype of *R. kochi* from Cluj-Napoca and the holotype of *R. filholi elongatum* from Pernes. The species "*R.*" *brevirostre* (= "*R.*" *orientale* according to Antoine *et al*. 2003) was excluded from the analysis because of the very scarce remains preserved (only a few fragmentary lower jaws are known). From the few observable characters and their dimensions, we suggest that this species should be excluded from *Ronzotherium* (presence of well-developed i1, of an isolated entoconid on p3–4 and of a keel below the symphysis in specimens illustrated by Dashzeveg 1991).

The other ronzothere terminals were chosen according to the completeness of the remains, and to their age, to represent as much as possible the morphological diversity through time. Therefore, we included specimens from Kleinblauen (MP21; Switzerland), Villebramar (MP22; France), Vendèze (MP24, France), Poillat (MP24, Switzerland), Bumbach (MP25, Switzerland), St-Henri/St-André/Les-Milles (= 'Marseille'; MP26, France), Gaimersheim (MP27, Germany), Rickenbach (MP29, Switzerland) as well as Lamothe-Capdeville (late early Oligocene, France) and 'Auvergne' (early Oligocene, France).

To test the monophyly of *Ronzotherium* and to understand its systematic position within the early Rhinocerotidae, we included a branching group (see Antoine 2002), comprising some of the earliest known Rhinocerotidae: the Late Eocene North American taxa *Teletaceras radinskyi* Hanson, 1989, *Penetrigonias dakotensis* (Peterson, 1920), *Trigonias osborni* Lucas, 1900 and representatives of *Epiaceratherium* Abel, 1910, comprising the Asian *E. naduongense* Böhme, Aiglstorfer, Antoine, Appel, Havlik, Métais, Laq, Schneider, Setzer, Tappert, Dang, Uhl & Prieto, 2013 and the European *E. bolcense* Abel, 1910, *E. magnum* Uhlig, 1999 and *E. delemontense* (Becker & Antoine, 2013), according to Tissier *et al.* (2020). We also included rhinocerotids ranging from the Oligocene to the earliest Miocene: *Molassitherium albigense* (Roman, 1912), *Mesaceratherium gaimersheimense* Heissig, 1969, *M. welcommi* Antoine & Downing, 2010 and *M. paulhiacense* (Richard, 1937), *Pleuroceros pleuroceros* (Duvernoy, 1853) and *P. blanfordi* Lydekker, 1884, *Protaceratherium minutum* Abel, 1910, *Subhyracodon occidentalis* (Leidy, 1850), *Diceratherium armatum* Marsh, 1875 and *Diaceratherium tomerdingense* Dietrich, 1931. Finally, we used *Uintaceras radinskyi* Holbrook & Lucas, 1997 from the late Middle Eocene of North America as outgroup of our study, because it is either considered as the

closest sister group to Rhinocerotidae (Prothero 2005), or as belonging to another rhinocerotoid family (Wang *et al.* 2016; Tissier *et al.* 2018).

The characters matrix is based on the matrix from Antoine (2002), and is provided in Supp. file 3. All characters except 72, 94, 102, 103, 140, 187 and 190 were considered to form morphoclines and were ordered ('additive') during the parsimony analysis. Six new characters were added:

283: p3, lingual branch of the paralophid: 0, developed; 1, reduced
284: p3–4, anterolingual cingulum: 0, stopping at the anterior valley or absent; 1, joining metaconid
285: P2, metacone fold: 0, strong; 1, weak or absent
286: P3–4, metacone fold: 0, strong; 1, weak or absent
287: M1–2, parastyle: 0, long; 1, short
288: I1, shape: 0, spatulate; 1, conical and pointed; 2, chisel (ordered)

We modified characters 2 and 3 from the original matrix of Antoine (2002) as follows:

2: Maxilla: foramen infraorbitalis: 0, above P1–2; 1, above P3; 2, above P4; 3, above molars
3: Nasal notch: 0, above P1–2; 1, above P3; 2, above P4–M1

Parsimony analyses were computed with the software PAUP* ver. 4.0a (build 167) (Swofford 2002). We used the heuristic search algorithm, with a random addition sequence of 1000 replicates and held 100 trees at each step, with a TBR swapping algorithm with no reconnection limit and swapping on all trees.

The analyses were performed by incrementing the new taxa, to test the reliability of the nodes and their behaviour to the addition of new terminals. When terminals not representing a type specimen were systematically found together in the most parsimonious tree (or strict consensus), even after the addition of new terminals, we decided to merge them together into a single terminal, thus representing the same species. When originally distinct, the scores of these terminals were considered as polymorphism after merging. The taxonomic sampling of the first analysis included only ronzotheres and the outgroup (*Uintaceras radinskyi*). The detailed protocol of the terminals addition and mergings and their results are reported in Table 1. The final resulting consensus tree is presented in the Results. In addition, a 100 bootstrap replicates were performed, retaining groups with frequency over 50% and decay index (Bremer) was calculated with the script for PAUP created by TreeRot ver. 3 (Sorenson & Franzosan 2007).

The results of these analyses are further discussed in the Results section below.

Systematics and comparison

The systematics provided here directly stem from our phylogenetic results. Emended diagnoses are provided and are also based on this phylogeny. All type specimens of each species of *Ronzotherium* are described in the Systematics section. In addition to these type specimens, all specimens from Ronzon assigned to *Ronzotherium velaunum* (type species of the genus) are described and illustrated, mostly for the first time. Postcranial remains from the Phosphorites du Quercy are tentatively attributed to *Ronzotherium filholi* and are also described and illustrated for the first time. These specimens provide complementary morphological comparisons of the postcranial anatomy of *Ronzotherium*. The holotype of *Ronzotherium kochi* Kretzoi, 1940, now synonymised with *Ronzotherium filholi*, is also illustrated, due to the scarcity of illustrations of this specimen in the literature. Recently found specimens from Poillat (Jura Canton, Switzerland) attributed to *Ronzotherium romani* are also described and illustrated for the first time. Moreover, we provide illustrations and descriptions of unpublished postcranial remains from Gaimersheim (Germany) which we refer to *R. romani*, and which unambiguously support its synonymy with *Diaceratherium massiliae* Ménouret & Guérin, 2009. For this reason, we also illustrate and describe all other known postcranial remains attributed to *R. romani*, i.e., those from the localities of 'Marseille' and Rickenbach. To support this synonymy and discriminate *R. romani* from *Diaceratherium*, we also compare these postcranial remains with other species of *Ronzotherium*, and with species of *Diaceratherium*. Finally, recently restored specimens from Bumbach attributed to *R. heissigi* sp. nov. are also illustrated and described for the first time. A list of comparative material used in this study is provided in the Appendix.

Table 1 (continued on next page). Terminals used during each parsimony analysis and their results. Names in bold correspond to terminals that frequently appear as sister groups and could be merged into a single terminal. Abbreviations: RI = retention index; CI = consistency index.

Taxa added	Terminals merged	Number of trees found	Results from the strict consensus for *Ronzotherium*	CI/RI
–	–	2	(*R. filholi*, Villebramar) (***R. elongatum*, Kleinblauen**) (Poillat (**'Marseille' (Rickenbach (*R. romani*, Gaimersheim)**)))	0.67/0.50
Teletaceras radinskyi	–	1	(*R. kochi* (*R. filholi*, Villebramar) (Poillat ((Vendèze (Lamothe (Auvergne, Bumbach))) ((***R. elongatum*, Kleinblauen**) (**'Marseille' (Rickenbach (*R. romani*, Gaimersheim)**))))	0.65/0.48
Penetrigonias dakotensis	–	8	(***R. elongatum*, Kleinblauen**) (Poillat (**'Marseille' (Rickenbach (*R. romani*, Gaimersheim)**)))	0.63/0.50
–	***R. elongatum*, Kleinblauen**	4	(Poillat (**'Marseille' (Rickenbach (*R. romani*, Gaimersheim)**)))	0.64/0.50
Trigonias osborni	–	19	(**'Marseille', Rickenbach, *R. romani*, Gaimersheim**)	0.61/0.49
–	***R. romani*, Rickenbach, Gaimersheim, 'Marseille'**	2	(***R. filholi*, Villebramar**) (**Auvergne, Bumbach**)	0.67/0.52
Epiaceratherium naduongense	–	2	Identical	0.64/0.51
Epiaceratherium bolcense	–	1	(*R. velaunum* (*R. elongatum* (*R. romani* ((Vendèze, Lamothe) ((***R. filholi*, Villebramar**) ((*R. kochi*, Poillat) ((**Auvergne, Bumbach**))))))))	0.62/0.50
–	**Auvergne, Bumbach (= *R.* indet.)**	24	–	0.63/0.50
Epiaceratherium magnum	–	23	–	0.60/0.51
Subhyracodon occidentalis	–	2	(*R. elongatum* (***R. filholi,* Villebramar**) ((***R. romani*, Poillat**)(**Vendèze (*R.* indet., Lamothe**)))	0.56/0.48
Epiaceratherium delemontense	–	2	Identical	0.56/0.50
Molassitherium albigense	–	5	((***R. romani*, Poillat**) (**Vendèze (*R.* indet., Lamothe**)))	0.53/0.49
Diceratherium armatum	–	2	(*R. elongatum* (***R. filholi,* Villebramar**) ((***R. romani*, Poillat**)(**Vendèze (*R.* indet., Lamothe**)))	0.49/0.48
–	***R. romani,* Poillat**	1	((*R. elongatum* (***R. filholi*, Villebramar**)) (*R. romani* (**Vendèze (Lamothe, *R.* indet.)**)))	0.50/0.49

Table 1 (continued). Terminals used during each parsimony analysis and their results. Names in bold correspond to terminals that frequently appear as sister groups and could be merged into a single terminal. Abbreviations: RI = retention index; CI = consistency index.

Taxa added	Terminals merged	Number of trees found	Results from the strict consensus for *Ronzotherium*	CI/RI
Mesaceratherium gaimersheimense	–	2	(*R. velaunum* (((*R. elongatum* (***R. filholi*, Villebramar**)) (*R. romani* (**Vendèze (Lamothe, *R.* indet.)**)))))	0.48/0.47
Pleuroceros pleuroceros	–	6	(((*R. elongatum* (***R. filholi*, Villebramar**)) (*R. romani* (**Vendèze (Lamothe, *R.* indet.)**))))	0.46/0.47
–	***R. filholi*, Villebramar**	6	((*R. elongatum, R. filholi*) (*R. romani* (**Vendèze (Lamothe, *R.* indet.)**))))	0.47/0.46
–	***R.* indet., Vendèze, Lamothe (= *R.* sp. nov.)**	14	(*R. romani*, *R.* sp. nov.)	0.48/0.44
Diaceratherium tomerdingense	–	4	(*R. velaunum*, *R. elongatum* ((*R. romani*, *R.* sp. nov.)(*R. filholi*, *R. kochi*)))	0.46/0.43
Pleuroceros blanfordi	–	1	(*R. velaunum* (*R. elongatum* ((*R. romani*, *R.* sp. nov.)(*R. filholi*, *R. kochi*)))	0.45/0.44
Mesaceratherium welcommi	–	1	Identical	0.42/0.44
Protaceratherium minutum	–	1	Identical	0.41/0.44
Mesaceratherium paulhiacense	–	2	Identical	0.40/0.44

Species delimitation

Throughout this paper, we will consider that all specimens from a single locality represent a small portion of a population, and we use these units as terminals in the phylogenetic analysis. Therefore, several terminals in our tree can belong to a single species. We use the "Diagnosable and Monophyly" version of the "Phylogenetic Species Concept" (PSC3 in Mayden 1997) of species to define species a posteriori, after the parsimony analysis. With this concept, a species is defined as "the smallest diagnosable cluster of individual organisms forming a monophyletic group within which there is a parental pattern of ancestry and descent" (McKitrick & Zink 1988). Under the "Unified Species Concept" proposed by de Queiroz (2005, 2007), this would correspond to a species defined by two properties: diagnosability and monophyly, which is near the maximum number of properties obtainable by palaeontological data, since reproductive isolation, ecology, behaviour, and genetic data are mostly unavailable. Furthermore, if one of these diagnosable and monophyletic clusters includes the holotype of any species, we consider that the terminals of this clade do belong to that species. If several holotype specimens of different species are grouped within a same clade and cannot be differentiated, we consider them as synonyms following the taxonomical rule of priority. Finally, to avoid the multiplication of poorly diagnosed species, we favour the most inclusive clades as species, for practical reasons. Indeed, any terminal which has even just one autapomorphy could be considered as a new species, as it is diagnosable, but applying this rule would imply that we know the full extent of intraspecific variability, which is not the case, and would also make species practically unusable.

Results

Phylogeny

Several terminals have been merged, in agreement with the results of the parsimony analyses. From the first analyses, the holotype of *Ronzotherium filholi elongatum* was always found as sister group to the specimens from Kleinblauen. They have thus been merged quite early into a single terminal representing *R. elongatum*. Similarly, the specimens from 'Marseille' (= St-Henri, St-André and Les Milles), Gaimersheim, and Rickenbach were always found together with the specimens of *Ronzotherium romani* from the type locality of La Ferté-Alais, although after the addition of *Trigonias osborni*, their topology slightly differed, resulting in an unresolved polytomy in the strict consensus. Yet, they still remained together as a clade and were thus also merged in a single terminal, which supports the former identifications of these specimens by other authors (i.e., Heissig 1969 for Gaimersheim; Ménouret & Guérin 2009 for Marseille; Mennecart *et al*. 2012 for Rickenbach). Furthermore, this also highlights the synonymy of *Ronzotherium romani* with *Diaceratherium massiliae* Ménouret & Guérin, 2009, that we further detail in the Systematic palaeontology section.

After these two fusions, the specimens from Bumbach and Auvergne were systematically found as sister groups. They were thus merged, representing an indeterminate species of *Ronzotherium*. After that, and the addition of new terminals, two clades occurred systematically: one including *Ronzotherium romani* and the specimens from Poillat, and another comprising the specimen from Vendèze as sister group to '*Ronzotherium* indet.' + the specimen from Lamothe-Capdeville. This former clade was thus merged into a single terminal, representing *R. romani*, and a new clade then became predominant, comprising the holotype of *Ronzotherium filholi* and the specimens from Villebramar. These were thus merged, as was also supported by the identification of these specimens from Villebramar as *R. filholi* by Brunet (1979), after which the specimens from Vendèze and Lamothe-Capdeville were merged with the '*Ronzotherium* indet.' documenting a new species: *Ronzotherium heissigi* sp. nov.

The identification of a new species from the localities of Bumbach, Auvergne, Vendèze, and Lamothe-Capdeville is supported by eight unambiguous autapomorphies, including mandibular, dental and postcranial characters (see Fig. 1). *Ronzotherium romani* further differs from this new species by seven unambiguous autapomorphies. The specimens from Bumbach were originally assigned to *Ronzotherium elongatum* by Heissig (1969), an assumption which is not supported by our analyses, as these samples are never found as sister groups and *R. elongatum* notably differs by its strong and continuous cingulum on the cheek teeth. Likewise, the specimens from 'Auvergne' (exact locality unknown) were attributed to *R. velaunum* by the same author, which is not supported by our analyses. However, both Heissig (1969) and Brunet (1979) referred to the specimens from Lamothe-Capdeville (described by Roman 1912a) as *R. romani*, whereas the specimen from Vendèze was identified as *R. velaunum* by Heissig (1969) and as *R. romani* by Brunet (1979). Here, we show that these specimens both belong to the same species, *R. heissigi* sp. nov., which is furthermore the sister species to *R. romani*, which could explain such previous discrepancies.

The final tree is presented in Fig. 1 and results from the strict consensus tree of two equally most parsimonious trees of 704 steps with a retention index (RI) of 0.44 and a consistency index (CI) of 0.40. According to our results, *Ronzotherium* is monophyletic and is the closest sister group to the Rhinocerotinae, which include *Mesaceratherium* Heissig, 1969, *Molassitherium* Becker & Antoine, 2013, *Subhyracodon* Brandt, 1878, *Diceratherium* Marsh, 1875, *Diaceratherium* Dietrich,1931, *Protaceratherium* Abel, 1910 and *Pleuroceros* Roger, 1898. At the base of the tree, four genera are placed as stem Rhinocerotidae. Within those, *Epiaceratherium* Abel, 1910 is the most basal and is monophyletic, followed by the American *Trigonias* Lucas, 1900, *Teletaceras* Hanson, 1989 and *Penetrigonias* Tanner & Martin, 1976. The nodes are overall quite poorly supported, either by Bremer values or bootstrap, which indicates high levels of homoplasy.

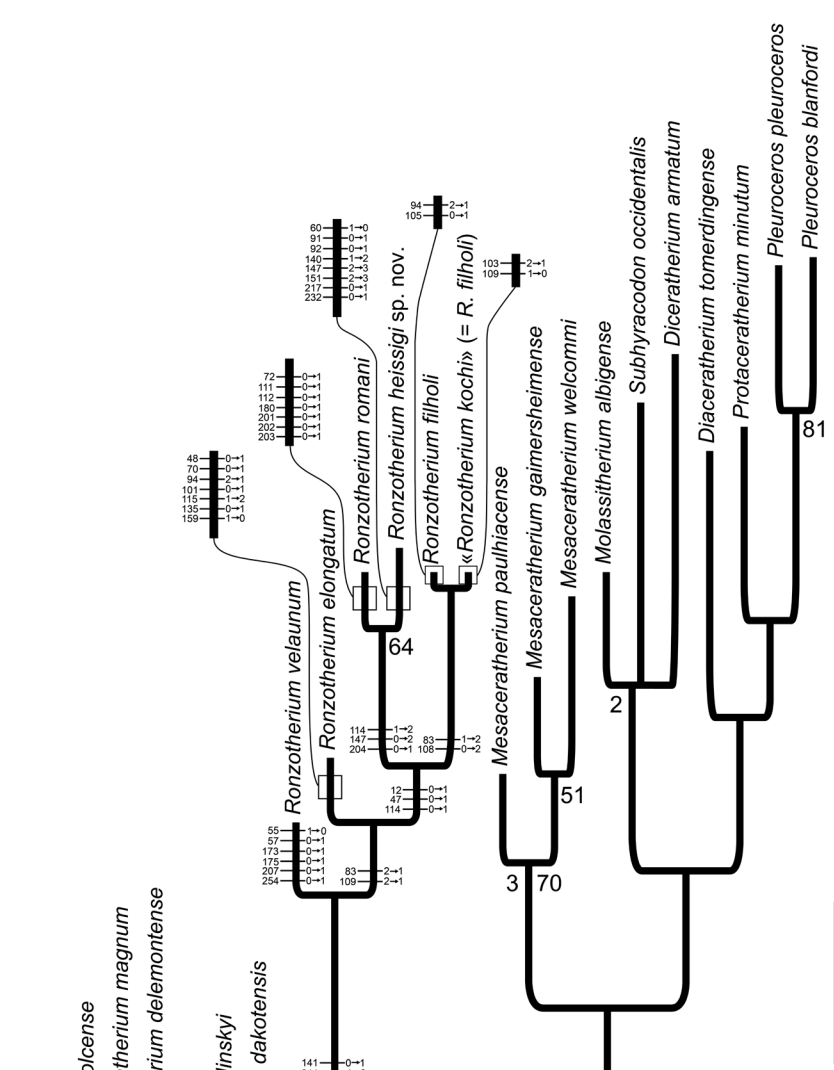

Fig. 1. Strict consensus of two equiparsimonious trees, inferred from a cladistic analysis of 288 morphological characters (length = 704 steps, RI = 0.44, CI = 0.40) and 24 rhinocerotid taxa. Numbers at nodes at the left of branches are decay index above 1, while numbers on the right of branches are bootstrap values above 50. Unambiguous synapomorphies of species of *Ronzotherium* Aymard, 1854 are reported on branches, with character numbers on the left and characters states changes on the right. Branch lengths are proportional to the number of transformations with ACCTRAN optimisation, the scale represents 20 steps.

Based on these results, *Ronzotherium* could comprise six species: *R. velaunum*, *R. elongatum*, *R. romani*, *R. heissigi* sp. nov., *R. filholi* and *R. kochi*. However, *R. filholi* and *R. kochi* only differ from each other by four unambiguous autapomorphies (two for each species), which is very poor to differentiate them. Thus, we suggest that they should actually be synonymized, pending more material from *R. kochi* is discovered, as it is currently only represented by a single maxilla with P2–M3.

Systematic palaeontology

Order Perissodactyla Owen, 1848
Superfamily Rhinocerotoidea Owen, 1845
Family Rhinocerotidae Gray, 1821

Genus ***Ronzotherium*** Aymard, 1854

Type species

Ronzotherium velaunum (Aymard in Pictet, 1853)

Other species

Ronzotherium filholi (Osborn, 1900); *Ronzotherium romani* Kretzoi, 1940; *Ronzotherium elongatum* Heissig, 1969; *Ronzotherium heissigi* sp. nov.

Emended diagnosis

These are large-sized hornless rhinocerotoids with two pointed upper incisors (I1 and I2) but only one large tusk-shaped lower incisor (i2) and without canines. The crown of the i1 is reduced. The dorsal profile of the skull is concave. The nasal incision is short and opening above P1–3. The anterior border of the orbit is above the molars and the infraorbital foramen is above P3–4. The processus posttympanicus and paraoccipitalis are fused at their base. The upper premolars are not molarised and the hypocone is always connected or completely fused to the protocone on P3–4. The upper molars are simple, with poorly developed crochet and antecrochet and the crista is always absent. The posterior part of the ectoloph of the upper molars is straight. The M3 is quadrangular in occlusal view. The ectoloph and metaloph are fused into an ectometaloph on M3, and there is no metastyle, but a posterior groove remains. The entoconid is very poorly developed on the lower premolars, or completely absent, and the opening of the posterior valley is wide and U-shaped. The lower d1 is usually absent. The ectolophid groove of the lower molars is developed until the neck. The distal articulation of the pyramidal for the lunate is symmetrical in medial view, the indentation on the medial side of the magnum is absent and the posterior tuberosity of the magnum is short. The collum tali of the astragalus is high.

Stratigraphical distribution

Late Eocene (?) to latest Oligocene.

Geographical distribution

Europe.

Ronzotherium velaunum (Aymard in Pictet, 1853)
Figs 2–7

Acerotherium velaunum Aymard in Pictet, 1853: 296.
Ronzotherium cuvieri Aymard, 1856: 233.

Rhinoceros velaunus – Aymard in Pictet 1853: 298.
Rhinocéros à incisives (*Ronzotherium*) – Aymard 1854: 675.
Ronzotherium velaunum – Aymard 1856: 233. — Filhol 1881: 3. — Osborn 1900: 232–237, 241, fig. 3. — Deninger 1903: 94–95. — Stehlin 1909: 509. — Abel 1910: 4–6, 8–9, 18, 33. — Roman 1912a: 4–5, 8, 10. — Kafka 1913: 5, 47, fig. 40a. — Airaghi 1925: 25. — Heissig 1969: figs 6a, 8c, 9a, 10a, 11, 25a (from Ronzon). — Brunet 1977: 16, 23; 1979: 102–104, 152–153, table 51, pls XV, XIXa–f. — Brunet *et al*. 1977: 109–112. — Jehenne & Brunet 1992: 202–203. — Uhlig 1996: 140–142. — Ménouret & Guérin 2009: 293–327. — Becker 2009: 495, 500.
Ronzotherium cuvieri (?) – Filhol 1881: 3.
Acerotherium velaunum – Filhol 1881: 75–78, figs 69–86, 88. — Mermier 1895: 176, 180, 186. — Roman 1910: 1558–1560; 1912a: 7, 27, 42–45, 56, 78, fig. 13, pl. II figs 2, 2a. — Gignoux 1928: 147, 149, 151.
Acerotherium cuvieri – Filhol 1881: fig. 87, 89–90. — Airaghi 1925: 26, 29.
? *Ronzotherium* cf. *velaunum* – Schlossser 1902: 112–113, pl. V figs 23, 25.
Rhinoceros velaunus – Roman 1912a: 45.
? *Ronzotherium velaunum* – Kafka 1913: 48–50, figs 40b, 41. — Kretzoi 1940: 89–92, 97–98, figs 1–2. — Lavocat 1951: 115. — Balme 2000: 153. — Costeur & Guérin 2001: 77.
Rhinoceros velaunum – Airaghi 1925: 32–33, 40–41.
Ronzotherium cf. *velaunum* – Heissig 1978: 249.

Non *Ronzotherium filholi* – Lavocat 1951: 116, pl. 19 fig. 3, pl. 26 fig. 1 (from Vendèze).
Non *Ronzotherium velaunum* – Heissig 1969: figs 5, 6b–d, 7, 8a–b, d–g, 9b–c, 10b–d, 25b (from ‘Auvergne’, Mouillac, Vendèze, St-Henri, St-André, Marseille, Les Milles).

Historical diagnoses

The first diagnosis of the species was provided by Heissig (1969, translated by the authors): “type species of the genus *Ronzotherium* with almost parallel i2 facing forward; i1 absent, I1 and I2 large. Lower jaw branches at an acute angle to each other. Upper molars broad, with long postfossette, narrow, slightly curved medisinus, thick and far forward paracone and mostly weak or missing lingual cingulum; M3 with sharp, narrow ectoloph edge behind the metacone. Upper premolars with straight or barely curved, parallel, originally slightly inclined transverse lophs and strongly waved lingual cingulum, slowly reduced; reduction begins at P4. P2 semimolariform to molariform, P3 and P4 premolariform to submolariform, but with relatively far apart inner lophs. Lower molars broad with weak labial cingulum; lower premolars with long talonid, mostly groove-shaped talonid pit and sharp, deep external groove. The entoconid lies far back, the cingulum is weak. The p1 is single rooted or missing.”

An emended diagnosis was provided by Brunet (1979, translated by the authors): “Stratigraphically the most ancient and primitive species of its kind. Skull: unknown. Mandible: posterior border of the symphysis just ahead of the d1, its lower surface presents a hull; very strong occlusion between i1 and i2. Decidual teeth: the upper milk premolars are unknown; the inferiors have a strongly curved hypolophid; d1 is biradiculate; the first lobe of d2 is strong with a long lingual branch of the paralophid, the ‘metaconid’ is not individualized; the anterior lobe of d3 is strong with a very long anterior branch of the paralophid. Definitive dentition: probable presence of i1. Upper premolars with a short postfossette, located above the posterior cingulum; strong lingual cingulum, barely waved. Upper molars with strong lingual cingulum, complete or disappearing only at the level of the hypocone. Lower premolars and molars: more or less large with a strong labial cingulum, more or less complete; the very notched talonid fossae on the labial side of the hypolophid are flatter, more horizontal, and lingually higher than in *R. filholi*; the trigonid fossae also open higher, above the anterolingual cingulum; premolars with long paralophid, without protoconid fold; P2 not reduced, with a strong anterolabial groove. Appendicular skeleton: tetradactyl hand with a gracile McV, reduced but complete; on the dorsal side of the hand, the

lunate articulates with the magnum; on the pyramidal, the ulnar facet is more laterally widened and the lower facet for the lunate higher and larger than in *R. filholi*; likewise, the magnum carries a much longer and higher facet for the McII."

Emended diagnosis

Type species of the genus with a posterior border of the symphysis located anterior to p2 and without lingual groove for the sulcus mylohyoideus on the corpus mandibulae. The metacone fold is present on M1–2. The d1 is absent in the juvenile, and the entoconid is constricted on decidual lower milk teeth. The cingula are poorly developed on upper and lower cheek teeth and discontinuous. The postero-proximal and anteroproximal facets for the lunate are in contact on the scaphoid and the fibula facet is oblique on the astragalus. The trapezium facet is absent on the McII.

Type material

Lectotype

FRANCE • right hemimandible still partly in sediment with poorly preserved p2–m3 and broken symphysis; Haute-Loire, near Le Puy-en-Velay, hill of Ronzon; PUY.2004.6.1765.RON.

Additional material

FRANCE • 1 broken mandible in several pieces, with i2 and p2–m3 on the left side and i2 and p2–(m1) on the right side; same collection data as for lectotype; PUY.2004.6.1766.RON • 1 juvenile mandible, still partly in sediment, with d2–d4 and erupting m1 on both sides and a small di1; same collection data as for lectotype; PUY.2004.7.1.RON • 1 broken ectoloph of P2?; same collection data as for lectotype; PUY.2004.6.1551.RON • 1 isolated P3; same collection data as for lectotype; PUY.2004.6.1767.RON • 1 isolated M1; same collection data as for lectotype; TLM.PAL.2010.0.122 • 1 cast of an isolated lower molar; same collection data as for lectotype; PUY.2004.6.841.RON • 1 distal part of humerus; same collection data as for lectotype; PUY.2004.6.262.RON • 1 complete scaphoid; same collection data as for lectotype; MNHN.F.RZN.503 • 1 lunate partly unextracted from sediment; same collection data as for lectotype; PUY.2004.6.1901.RON • 1 pyramidal, still in sediment; same collection data as for lectotype; MNHN.F.RZN.504 • 1 pyramidal; same collection data as for lectotype; MNHN.F.RZN.502 • 1 pisiforms, still in sediment; same collection data as for lectotype; MNHN.F.RZN.505 • 1 pisiforms, still in sediment; same collection data as for lectotype; PUY.2004.6.1901.RON • 1 magnum, still in sediment; same collection data as for lectotype; PUY.2004.6.907.RON • 1 magnum; same collection data as for lectotype; PUY.2004.6.263.RON • 1 broken anterior part of unciform; same collection data as for lectotype; PUY.2004.6.1480.RON • 2 distal parts of femora; same collection data as for lectotype; PUY.2004.6.266.RON, PUY.2004.6.267.RON • 2 proximal parts of tibiae; same collection data as for lectotype; PUY.2004.6.260.RON, PUY.2004.6.261.RON • 1 ectocuneiform, still partly in sediment; same collection data as for lectotype; PUY.2004.6.577.RON • 1 cuboid, still in sediment; same collection data as for lectotype; PUY.2004.6.1309.RON • 1 cuboid; same collection data as for lectotype; PUY.2004.6.268.RON • 1 astragalus, still preserved in sediment; same collection data as for lectotype; PUY.2004.6.1770.RON • 1 central metapodial, still in sediment; same collection data as for lectotype; PUY.2004.6.840.RON • 1 lateral phalanx, still in sediment; same collection data as for lectotype; PUY.2004.6.604.RON.

Type horizon and locality

Hill of Ronzon, near Le Puy-en-Velay (Haute-Loire, France), MP21 (early Oligocene).

Stratigraphical distribution

MP21 (early Oligocene).

Geographical distribution

France: Ronzon, Lagny-Torigny, Ruch. Germany: Haag 2, Möhren 20.

Description

Mandibles. Three mandibles of *R. velaunum* from Ronzon are preserved. The lectotype mandible PUY.2004.6.1765.RON is a right hemimandible with p2–m3 (Fig. 2A–D). The posterior part of the specimen and the symphysis are broken, and the left side is still in sediment. The base of the corpus mandibulae is straight and low, with a constant height below the teeth neck. The ramus is vertical, and the coronoid process is well developed and high. The mandible PUY.2004.6.1766.RON is badly preserved and in several pieces (Fig. 2E–J). The symphysis as well as both branches are preserved, with i2, the root of d1 and p2–m3 on the left side, and only i2 and p2–m1 on the right side. It was recently prepared and new characters can now be observed: the angle between the symphysis and the corpus is low, the symphysis is rather narrow and its posterior borders is in front of p2, the foramen mentale is below p2 and there is no lingual groove of the sulcus mylohyoideus. The last mandible PUY.2004.7.1.RON belonged to a juvenile individual and is still partly preserved in sediment (Fig. 2K–O). It bears d2–d4 and erupting m1 on both sides as well as a small di1 on the right side. There is apparently no dp1. The posterior border of the symphysis is anterior to d2. No lingual groove of the sulcus mylohyoideus is visible.

Upper dentition. Very few upper teeth are preserved in this locality (Fig. 3): an ectoloph of a left P2 (PUY.2004.6.1551.RON), a P3 (PUY.2004.6.1767.RON) and an M1 (TLM.PAL.2010.0.122). However, Filhol (1881) noted the existence of an upper maxilla that he could not have accessed during his study and was supposedly in Pichot-Dumazel's collection. Unfortunately, this maxilla remains unknown. The P2 and P3 have strong paracone and metacone folds and very thin discontinuous labial cingulum. Their crown is low. The lingual cingulum is strong and continuous on P3. The P3 is three-rooted and few characters can be observed, as it is very worn. Its postfossette is narrow and the protocone and hypocone were probably not separated. The M1 has four roots and is also much worn. Labial cingulum is almost completely absent. Lingual cingulum is strong and continuous under the protocone and disappears under the hypocone. The paracone fold is strong and the metacone fold is present but very thin. The parastyle is strong and there is no mesostyle. The protocone does not seem constricted. The posterior profile of the ectoloph is slightly concave.

Lower dentition. The definitive anterior dentition is only represented by two i2 from the mandible PUY.2004.6.1766.RON. They are straight and horizontal. The roots are wider than the crown, and the crown shows a clear and large wear-facet, which means that I1 and i2 could contact each other. The transverse outline of the crown is in the shape of a medially pinched drop. The neck is not marked and the enamel is very thin. The lower cheek teeth are two-rooted and low-crowned. There is no cement. The premolar row is short compared to the molar row ($0.42 < Lp3–4/Lm1–3 < 0.50$). A weak labial cingulum is sometimes present on the lower cheek teeth, but a lingual cingulum is always absent. Vertical external rugosities are present on the ectolophid of p2–3. The ectolophid groove is developed and does not vanish before the neck. In occlusal view, the trigonid is very angular and forms a right dihedron which becomes more acute with wear, while the talonid is rounded. The talonid basin of the lower premolars is poorly developed: the entoconid is completely absent and the hypoconid is low. The hypolophid vanishes before the posterolingual border of the premolars, the posterior valley is therefore very wide and U-shaped. On the contrary, the anterior valley is narrow, and both valleys open very high above the neck. The metaconid is the largest and most developed cusp on lower premolars. On p3, the metaconid bears an anterior crest, almost closing the anterior valley. The paralophid of premolars has two branches, a labial branch, and a high and long anterior branch, parallel to the protolophid. The molars greatly differ from the premolars by the much stronger development of the entoconid, which is also slightly constricted. The opening of the anterior valley is higher than the posterior one.

Fig. 2. *Ronzotherium velaunum* (Aymard in Pictet, 1853) from Ronzon (earliest Oligocene, France). – **A–D**. Lectotype right hemimandible PUY.2004.6.1765.RON with p2–m3. **A**. Lateral view. **B**. Medial view. **C**. Occlusal view. **D**. Drawing of the occlusal view. – **E–J**. Broken left hemimandible PUY.2004.6.1766. RON with i2 and p2–m3. **E**. Lateral view. **F**. Medial view. **G**. p4–m3 in occlusal view. **H**. Drawing of p4–m3. **I**. Symphysis with p2–3 in occlusal view. **J**. Drawing of p2–3. – **K–O**. Juvenile mandible PUY.2004.7.1.RON. **K**. di1, d2–d4 and erupting m1 in occlusal view. **L**. Right d2–4 in labial view. **M**. Left d4–m1 in lingual view. **N**. Left d2–4 in occlusal view. **O**. Right d2–4 in occlusal view. Scale bars: 2 cm.

Decidual dentition. Only the lower decidual dentition is known from Ronzon, from the juvenile mandible PUY.2004.7.1.RON (Fig. 2K–O). The di1 is very small and has a conical crown. There does not seem to be a d1 in the juveniles. However, d2–4 are well developed. The metaconid and entoconid are slightly constricted, especially on d4. There is neither a protoconid fold nor a vertical external rugosity. The lingual and labial cingulum are absent. The ectolophid fold is strong on d2 but there is no anterior groove on the ectolophid. The paralophid is double on d2–3 and simple on d4. On d2, the posterior valley is almost closed by the extension of the entoconid, but still narrowly open. There is no lingual groove of the entoconid on d3. The d4 is very molariform.

Humerus. One distal fragment of humerus is preserved (PUY.2004.6.262.RON, Fig. 4A–C). The fossa olecrani is high but not very deep. The distal articulation is well constricted and there is no scar on the trochlea. The distal gutter on the epicondyle is also absent. Medial and lateral epicondyles are poorly developed and the lateral epicondylar crest is weakly extended laterally.

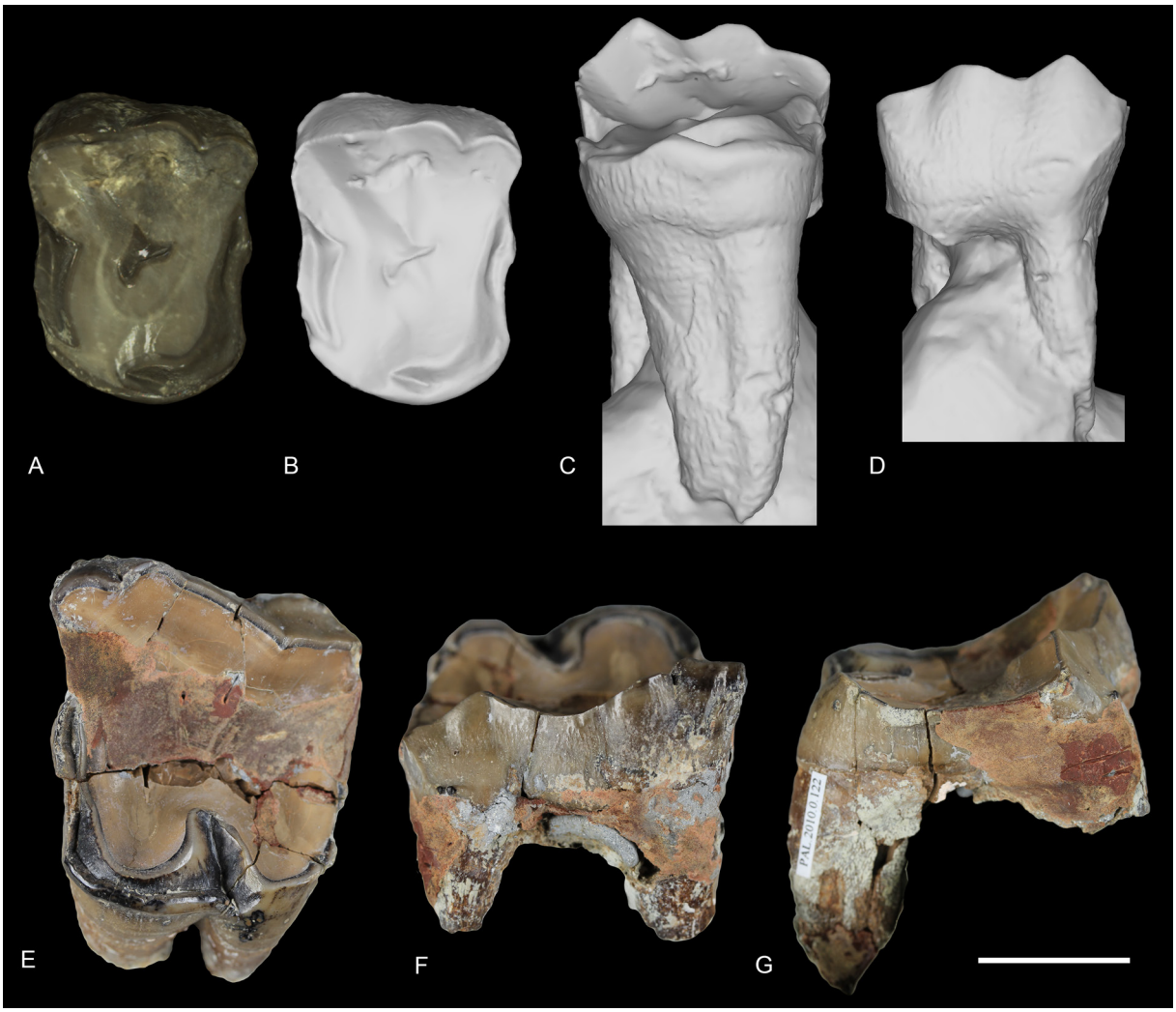

Fig. 3. *Ronzotherium velaunum* (Aymard in Pictet, 1853) from Ronzon (earliest Oligocene, France). – **A–D**. 3D surface scans of P3 PUY.2004.6.1767.RON. **A**. With texture in occlusal view. **B**. Without texture in occlusal view. **C**. Without texture in lingual view. **D**. Without texture in labial view. – **E–F**. M1 TLM.PAL.2010.0.122. **E**. Occlusal view. **F**. Labial view. **G**. Lateral view. Scale bar: 2 cm.

Fig. 4. *Ronzotherium velaunum* (Aymard in Pictet, 1853) from Ronzon (earliest Oligocene, France). – **A–C**. Left distal humerus PUY.2004.6.262.RON. **A**. Anterior view. **B**. Posterior view. **C**. Distal view. – **D–G**. Right scaphoid MNHN.F.RZN.503. **D**. Medial view. **E**. Lateral view. **F**. Proximal view. **G**. Distal view. – **H–J**. Right lunate PUY.2004.6.1901.RON. **H**. Anterior view. **I**. Lateral view. **J**. Proximal view. – **K–M**. Right pyramidal MNHN.F.RZN.502. **K**. Lateral view. **L**. Medial view. **M**. Posterior view. – **N**. Left pyramidal MNHN.F.RZN.504, distal view. Abbreviations: adl = anterodistal facet for the lunate; apl = anteroproximal facet for the lunate; l = lunate; le = lateral epicondyle; lec = lateral epicondylar crest; m = magnum; me = medial epicondyle; of = olecranon fossa; p = pyramidal; pi = pisiform; ppl = postero-proximal facet for the lunate; pt = posterior tuberosity; r = radius; s = scaphoid; td = trapezoid; tm = trapezium; u = ulna; un = unciform. Articular surfaces highlighted in white. Scale bars: 2 cm.

Scaphoid. The scaphoid MNHN.F.RZN.503 (Fig. 4D–G) is well preserved. The anterior height is equal to the posterior one. The postero-proximal articulation with the lunate bone is not visible but may have been present on the eroded proximo-lateral tuberosity and fused with the anteroproximal facet. The proximal facet for the radius is very concave and fuses anteriorly with the anteroproximal facet for the lunate bone. The anterodistal facet for the lunate is poorly distinguished. The three distal articular facets are concave in lateral view. The trapezium facet is rather large and triangular. The trapezoid facet is the largest and has a prominent dorso-medial extension. The magnum facet is concave in lateral view.

Lunate. The lunate bone PUY.2004.6.1901.RON (Fig. 4H–J) is still mostly concealed in the sedimentary block. Only the proximal, dorsal and lateral sides are visible. It is an overall large and robust bone. The posterior tuberosity is almost as wide as the proximal facet for the radius. Two articular facets are visible on the lateral side, both corresponding to the pyramidal bone. The proximal facet is small while the distal one is large, flat and circular. On the medial side, two well separated articular facets can be distinguished and correspond to the scaphoid, which implies the presence of a postero-proximal facet for the lunate on the scaphoid, that is not visible on the scaphoid MNHN.F.RZN.503.

Pyramidal. Two pyramidals are preserved (MNHN.F.RZN.502, Fig. 4K–M and MNHN.RZN.504, Fig. 4N). There are two proximal articulation facets: a large one for the ulna, and a smaller one, elongated and band-like for the pisiform. The medio-distal articulation for the lunate is symmetrical and the distal facet for the unciform is triangular.

Pisiform. The pisiform MNHN.RZN.505 is still in articulation with the pyramidal MNHN.RZN.504. Another unnumbered pisiform is preserved on the sedimentary bloc of the lunate bone PUY.2004.6.1901. RON. The pisiform is very small, and neither flattened nor elongated. It bears a large proximal articular facet for the radius. The distal end is roughly conical and rounded.

Unciform. Only the dorsal part of the left unciform PUY.2004.6.1480.RON is preserved, the posterior tuberosity is missing (Fig. 5F–G). There are two proximal facets: a large one, dorso-ventrally convex for the pyramidal, and smaller one, flattened and arrowhead-shaped for the lunate. They form an angle of 120–130° in dorsal view. The posterior expansion of the pyramidal facet is very short and wide. The three distal facets, for the magnum, McIII and McIV, are partially covered in sediment. The lateral McV facet is broken but was probably distinct from the pyramidal facet.

Magnum. Two magnums are preserved. PUY.2004.6.907.RON is still in a sedimentary bloc, while PUY.2004.6.263.RON is subcomplete and fully extracted (Fig. 5A–E). It is a rather tall bone, the proximodistal height is almost equal to the dorsoventral length, but it is very compressed transversally. In anterior view, the anterior border of the scaphoid facet is nearly straight. The lunate facet is very long dorsoventrally, and very convex proximally. There are two medial facets below the scaphoid facet: a proximal one for the trapezoid and a distal one for the McII. The former is trapezoidal while the latter is curved. There is no indentation between these two facets. The distal facet for the McIII is large and deeply concave dorsoventrally. The unciform facet on the lateral side is not preserved. The posterior tuberosity of the magnum is long, thin and curved.

Femur. There are two distal ends of left femora in Ronzon (PUY.2004.6.266.RON, Fig. 6A–D, I and PUY.2004.6.267.RON, Fig. 6E–H, J). In anterior view, the medial lip of the trochlea is prominent. The groove between the two trochlea is not very deep and the proximal border of the trochlea is almost straight. In lateral view, the medial lip of the trochlea is strongly forward compared to the diaphysis. In posterior view, the two condyles are similar in size and widely separated by the intercondylar fossa.

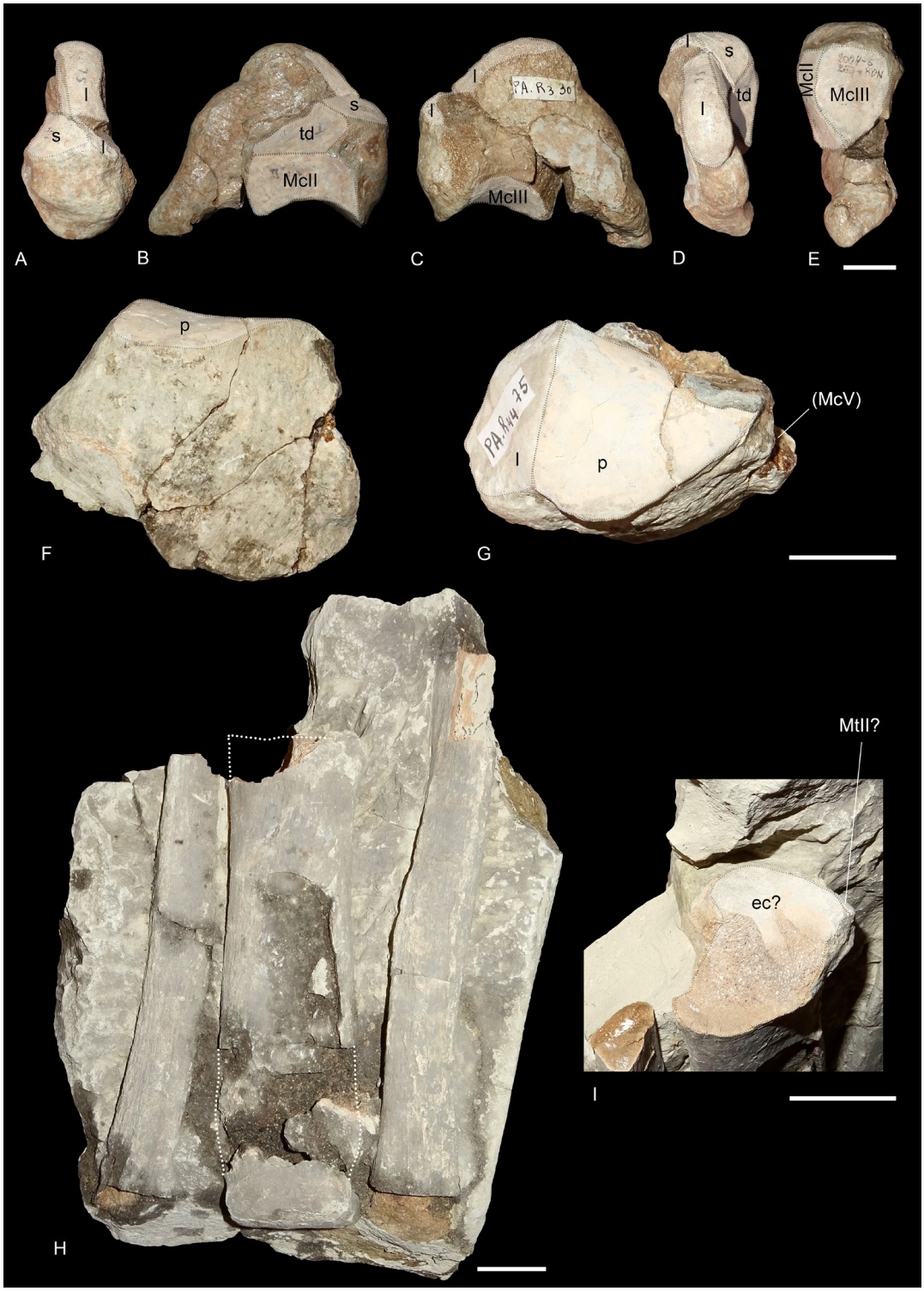

Fig. 5. *Ronzotherium velaunum* (Aymard in Pictet, 1853) from Ronzon (earliest Oligocene, France). – **A–E**. Left magnum PUY.2004.6.263.RON. **A**. Anterior view. **B**. Medial view. **C**. Lateral view. **D**. Proximal view. **E**. Distal view. – **F–G**. Left unciform PUY.2004.6.1480.RON. **F**. Anterior view. **G**. Proximal view. – **H–I**. Central metapodial PUY.2004.6.840.RON (possibly a MtIII) on sedimentary block, along with two probable ribs on its right and left. **H**. Anterior view. **I**. Close-up view of the proximal extremity. Abbreviations: ec = ectocuneiform; l = lunate; p = pyramidal; s = scaphoid; td = trapezoid. Articular surfaces highlighted in white. Scale bars: 2 cm.

The supracondylar fossa is shallow. In distal view, the articular surfaces of the trochlea and the condyles are connected medially and laterally.

Tibia. Two proximal ends of left tibias (PUY.2004.6.260.RON and PUY.2004.6.261.RON) could belong to the same individuals as the femora (Fig. 6K–P). In proximal view, it is wider than long. The tibial tuberosity is weakly developed and is laterally displaced. It is separated from the medial tuberosity by a wide groove. The cranial intercondylar area is deep and wide, the central one very small and the caudal one is deep and slender. The lateral condyle is oval, and wider than long, while the medial one is almost rectangular and longer than wide. In anterior view, the medial tuberosity is higher than the lateral one. In lateral view, the groove for the extensor is wide and shallow and the tibial fossa rather deep. The tibia and fibula were completely independent, there is no contact mark along the diaphysis, only a high articular facet below the lateral condyle.

Astragalus. Only the anterior face of the astragalus (PUY.2004.6.1770.RON) is visible, the other side is still in sediment, but it is complete (Fig. 7A–D). The transverse diameter/height (TD/H) ratio is slightly above 1, but below 1.2, whereas the anteroposterior diameter/height (APD/H) ratio is below 0.65. On the lateral side, the fibula facet is slightly oblique and flat. The collum tali is very high. There are two distal articular facets: the navicular facet is large and slightly concave transversally, while the facet for the cuboid is small and flat. In distal view, the trochlea is very oblique compared to the distal articulation. The medio distal tubercle is well developed.

Cuboid. Two cuboids are preserved: one is still partially in sediment (PUY.2004.6.1309.RON) but the other is subcomplete (PUY.2004.6.268.RON, Fig. 7I–M). The proximal articular surface is triangular. There are two distinct surfaces, for the astragalus and the calcaneus, distinguished by a shallow groove. The calcanear one is the largest. In anterior view, the bone is rectangular and higher than wide. In lateral view, the lateral groove for the tendons is very deep. The posterior apophysis is wide and stout, and extends more distally than the distal articular facet. The distal articulation surface for the MtIV is almost a right triangle with rounded edges.

Ectocuneiform. The right ectocuneiform PUY.2004.6.577.RON is still partially in sediment, the proximal side is not visible (Fig. 7E–H). The distal articular facet for the MtIII is crescent-shaped. The posterolateral process is rather short and medially oriented. The medial side is straight and bears three facets: one dorsal and band-shaped for the mesocuneiform, and two distal, oval-shaped for the MtII. The lateral side is curved and the two articulations postero-proximal and anterodistal for the cuboid are separated by a deep groove.

Metapodial. A central metapodial (PUY.2004.6.840.RON) is also preserved from Ronzon, still in sediment, and only the dorsal side is visible (Fig. 5H–I). The proximal articulation is very incomplete, but it is nonetheless rather dorsoventrally flat, which would indicate a MtIII rather than a McIII, as also suggested by Brunet (1979). There is a small anteroproximal facet for the MtII, the posterior one, if present is hidden by sediment. The diaphysis gets slightly wider towards the distal end. The median keel of the distal articulation is smooth.

Lost material. The scaphoid and pyramidal thought as lost by Brunet (1979) and figured by Filhol (1881) are now in fact in the collections of MNHN (Paris, France) (MNHN.F.RZN.502, MNHN.F.RZN.503 and MNHN.F.RZN.504). However, the calcaneum, MtIV and McV, figured by Filhol (1881: pl. 13), are indeed lost and could not be found either in the Musée Crozatier (Le Puy-en-Velay, France) or in the MNHN.

Fig. 6. *Ronzotherium velaunum* (Aymard in Pictet, 1853) from Ronzon (earliest Oligocene, France). – **A–D, I**. Left distal femur PUY.2004.6.266.RON. **A**. Anterior view. **B**. Posterior view. **C**. Lateral view. **D**. Medial view. **I**. Distal view. – **E–H, J**. Left distal femur PUY.2004.6.267.RON. **E**. Anterior view. **F**. Posterior view. **G**. Lateral view. **H**. Medial view. **J**. Distal view. – **K, M–N**. Left proximal tibia PUY.2004.6.261.RON. **K**. Proximal view. **M**. Anterior view. **N**. Posterior view. – **L, O–P.** Left proximal tibia PUY.2004.6.260.RON. **L**. Proximal view. **O**. Anterior view. **P**. Posterior view. Abbreviations: aia = anterior intercondylar area; icf = intercondylar fossa; lc = lateral condyle; ll = lateral lip of the trochlea; mc = medial condyle; ml = medial lip of the trochlea; pia = posterior intercondylar area; tt = tibial tuberosity. Articular surfaces highlighted in white. Scale bar: 2 cm.

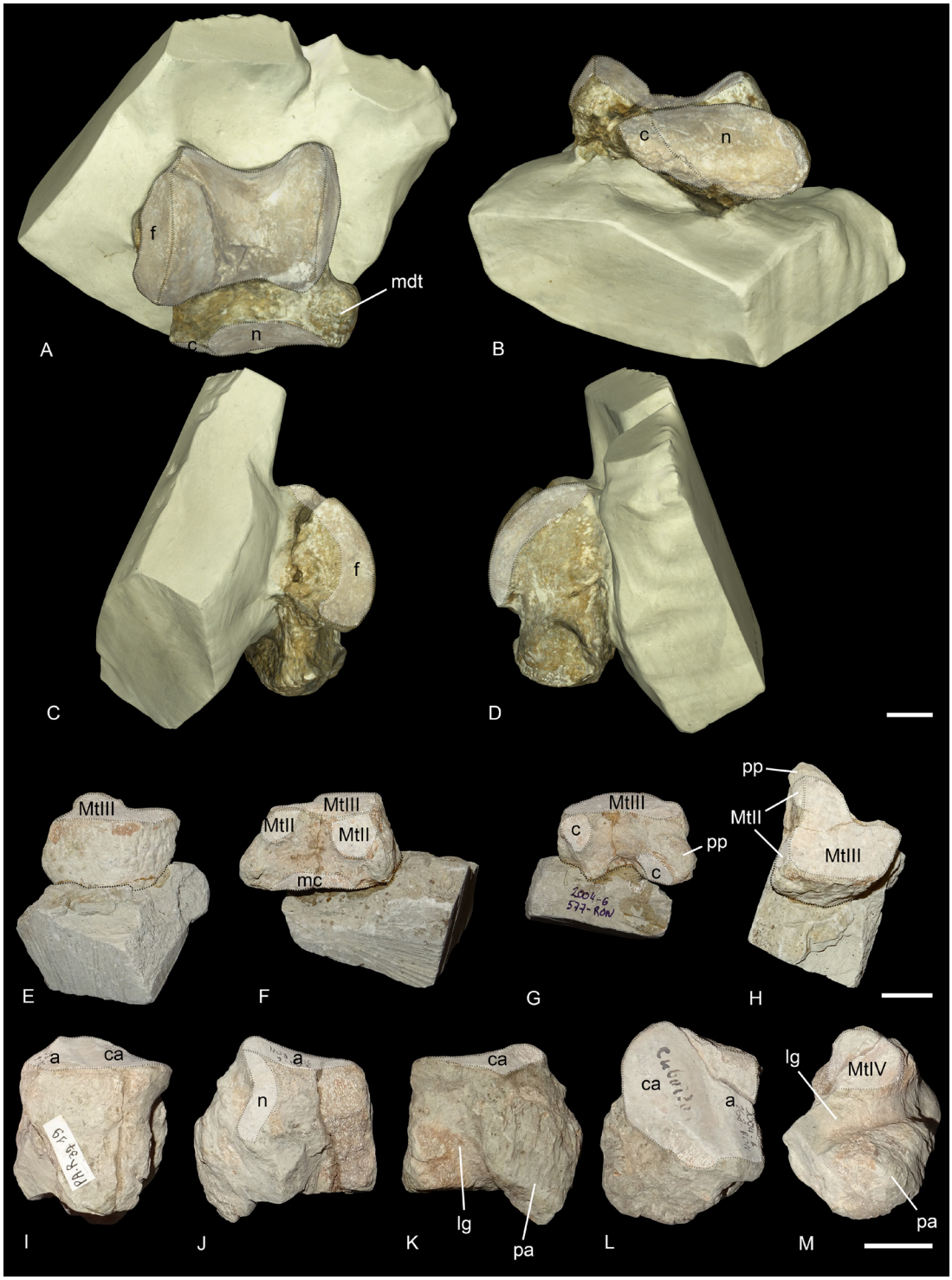

Fig. 7. *Ronzotherium velaunum* (Aymard in Pictet, 1853) from Ronzon (earliest Oligocene, France). – **A–D**. Right astragalus PUY.2004.6.1770.RON. **A**. Anterior view. **B**. Distal view. **C**. Lateral view. **D**. Medial view. – **E–H**. Right ectocuneiform PUY.2004.6.577.RON. **E**. Anterior view. **F**. Medial view. **G**. Posterior view. **H**. With distal border towards the top, and distal view. – **I–M**. Left cuboid PUY.2004.6.268.RON. **I**. Anterior view. **J**. Medial view. **K**. Lateral view. **L**. Proximal view. **M**. Distal view. Abbreviations: a = astragalus; c = cuboid; ca = calcaneus; f = fibula; lg = lateral groove; mc = mesocuneiform; mdt = medio-distal tubercle; n = navicular; pa = posterior apophysis; pp = posterolateral process. Articular surfaces highlighted in white. Scale bars: 2 cm.

Ronzotherium elongatum Heissig, 1969
Figs 8–10

Ronzotherium filholi elongatum Heissig, 1969: 46–55, 68, 71, 116, 119, fig. 18d (from Pernes and Kleinblauen).

Rhinoceros filholi – Jenny 1905: 125.
Aceratherium filholi – Jenny 1905: 125. — Roman 1910: 1559 (from Pernes and Kleinblauen); 1912a: 17, 27, 45–50, 57–58, figs 14.1, 15, 18, pl. V figs 1–2 (from Pernes and Kleinblauen); 1912b: 360–364, fig. 2. — Stehlin 1914: 185 (from Kleinblauen). — Gignoux 1928: 148, 151, fig. 3 (from Pernes and Kleinblauen).
Praeaceratherium filholi – Spillmann 1969: figs 11, 13, 16.
Ronzotherium filholi – Brunet 1979: 105, table 2 (from Pernes and Kleinblauen). — Becker 2003: 212–213, 230–231, 234, 256, pl. II fig. a–d (from Kleinblauen); 2009: 490, 493–495, fig. 4h–l, table 1 (from Kleinblauen). — Ménouret & Guérin 2009: 296 (from Pernes and Kleinblauen).

Non *Ronzotherium filholi elongatum* – Heissig 1969: 46–55, figs 16–17, 18a–c, 19 (from Villebramar, Bumbach, Montans, Cournon).

Historical diagnosis

From Heissig (1969), translated by the authors: "A subspecies of *Ronzotherium filholi* with the following characteristics: corpus mandibulae low, very slender, fossa masseterica deeply concave, foramen mandibulae at about the level of the teeth neck, strongly enlarged, symphysis long, flat forward; i2 still shearing towards I1, i1 present; angle of jaw branches very pointed; upper molars elongated with very broad medisinus, extremely short post-fossette and strong lingual cingulum; upper P3 and P4 premolariform to semimolariform, P2 molariform, protocone and hypocone widely separated, all upper premolars strongly widened, inside slightly rounded, metaloph curved and S-shaped, often with complicated folds, hypostyle missing; lower molars with strong labial cingulum and relatively long anterolingual cingulum, relatively long, narrow and conspicuously low, talonid pit unclear or notched; lower premolars, especially p3 often lengthened to the front, protoconid fold strong, metalophid strongly backwards, labial cingulum strong, p2 strongly narrowed, p1 single-rooted."

However, this diagnosis is not only based on the type material, but also on referred material from other localities, such as Villebramar or Bumbach that we refer to other species. We thus propose an emended diagnosis.

Emended diagnosis

The paraoccipital process is poorly developed. The roots of the upper cheek teeth are lingually fused, P2 is molariform with a lingual bridge connecting the protocone and hypocone, the protocone and hypocone form a lingual wall on P3 and P4, with a well-marked lingual groove above the cingulum, especially on P4. Upper premolars usually bear a simple crochet, the protocone is slightly constricted, the metaloph curved and S-shaped and the hypostyle missing. The protocone is usually constricted on upper molars and the lingual cingulum is strong and continuous, except under the hypocone of M1–2 and the protocone of M2. The labial cingulum of the lower molars is always present and continuous.

Differs from *Ronzotherium filholi* by the presence of a processus postorbitalis on the zygomatic arch and by its poorly developed processus paraoccipitalis.

Type material

Holotype

FRANCE • two-parts well preserved skull with almost complete cheek teeth rows, the two parts are joined together by plaster, which does not reflect the original morphology; Vaucluse, Pernes-les-Fontaines; probably MP23; FSL-9601.

Additional material

No other material is known from this locality.

Type horizon and locality

Pernes (= Pernes-les-Fontaines, Vaucluse, France), probably dated from MP23. The 'sands and green sandstones of the Valette-de-Pernes' in which this skull was found, have been dated from MP23 in Murs, another locality 20 km from Pernes.

Stratigraphical distribution

Early Oligocene.

Geographical distribution

France: Pernes. Switzerland: Kleinblauen.

Description

Skull. The skull was originally described by Roman (1912a, 1912b), who attributed it to *Ronzotherium filholi*. It is heavily reconstructed in plaster, especially the frontals and parietals, but it is nonetheless possible to identify the original bony material (Figs 8–9). The nasals are very fragmentary, the anterior part is broken. The lateral apophysis is not preserved. The infraorbital foramen opens above P4. The posterior border of the nasal incision is above P3 and the anterior border of the orbit is above the middle of M1. The lachrymal process is well developed and there is a large postorbital process of the frontals above the orbit. Only the anterior parts of the jugal bones are preserved, and the anterior base of the zygomatic arch is high above the teeth neck. The postorbital process of the zygomatic arch is large and on the jugal. The squamosals are not preserved. The dorsal profile of the skull is difficult to interpret, because of the heavy reconstruction, yet it was probably concave, though not as much as suggested by the reconstruction. The area between the temporal and nuchal crests is very concave. The external auditory pseudomeatus is ventrally open, between the postglenoid and posttympanic apophyses. The nuchal tubercle is well-developed. From the preserved part of the parietal bone, we can observe a wide parietal crest. The occipital crest is concave. In ventral view, the anterior part of the zygomatic arch does not strongly diverge from the maxilla. The vomer is badly preserved. The articular tubercle of the squamosal is smooth and tranversally straight. The postglenoid apophysis is rounded and convex anteriorly, and anteroposteriorly elongated. The foramen nervi hypoglossi is in the middle of the condylar fossa. There is a strong and high sagittal crest on the basilar process of the basioccipital. In occipital view, the paraoccipital and posttympanic processes are fused. The posttympanic process is well-developed and the paraoccipital process is partly broken. The foramen magnum is circular. There is neither a median crest nor a medial truncation on the occipital condyles.

Upper cheek teeth. No anterior teeth are preserved on the skull, only the cheek teeth (Figs 8B–C, 9B–C, 10C–D). The three molars are well preserved on both sides, but the ectolophs of P3–4 are missing, whereas P2 is well preserved and P1 is absent on both sides. There is, however, a single broken root still preserved on the left side which means that this tooth was present in the juvenile at least. The premolar series is short compared to the molar series (LP3–4/LM1–3 = 0.48). There are no enamel folds and the cement is absent. The crown of the cheek teeth is low.

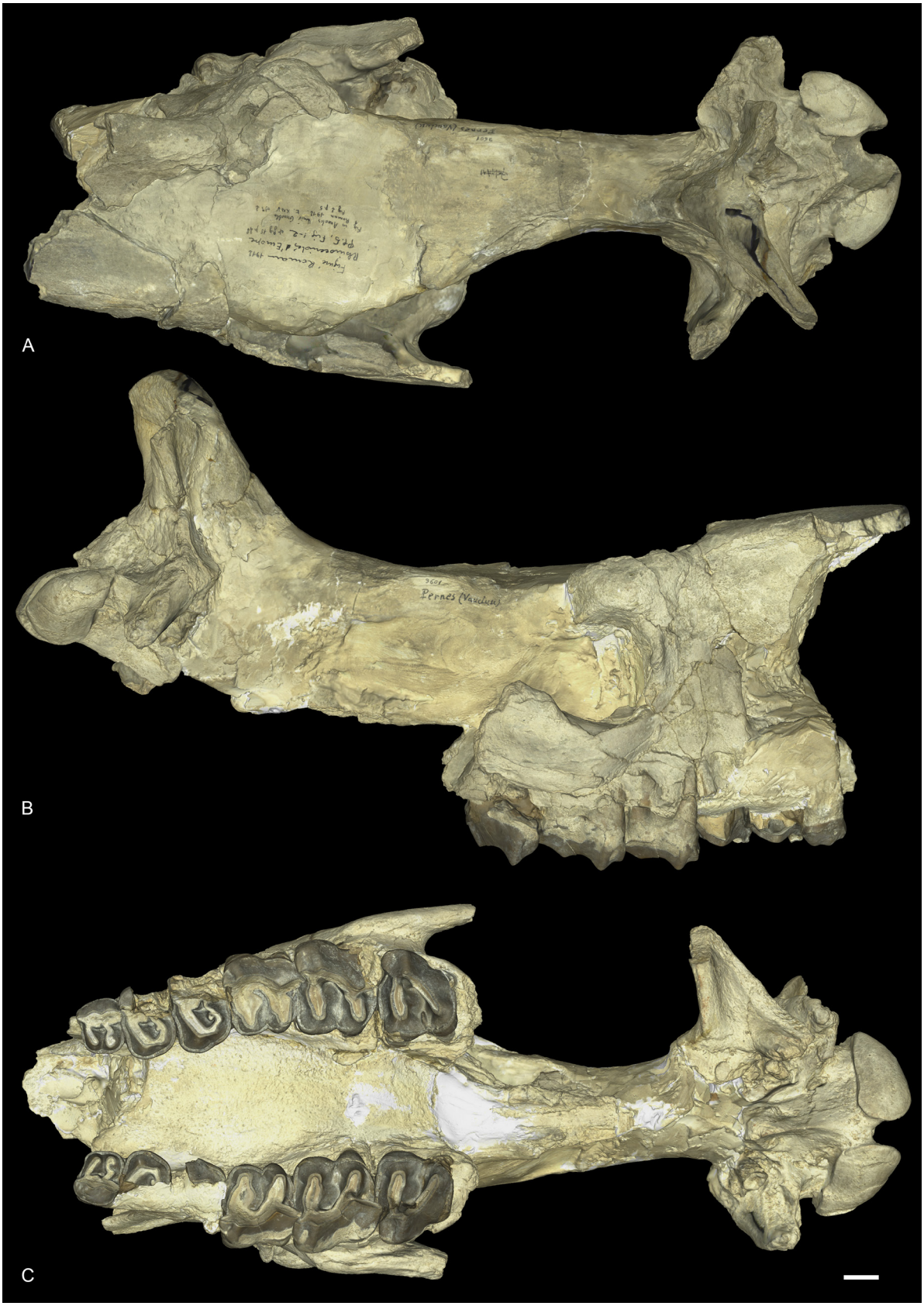

Fig. 8. *Ronzotherium elongatum* Heissig, 1969 from Pernes (early Oligocene?). Skull FSL-9601. **A**. Dorsal view. **B**. Right lateral view. **C**. Ventral view. Scale bar: 2 cm.

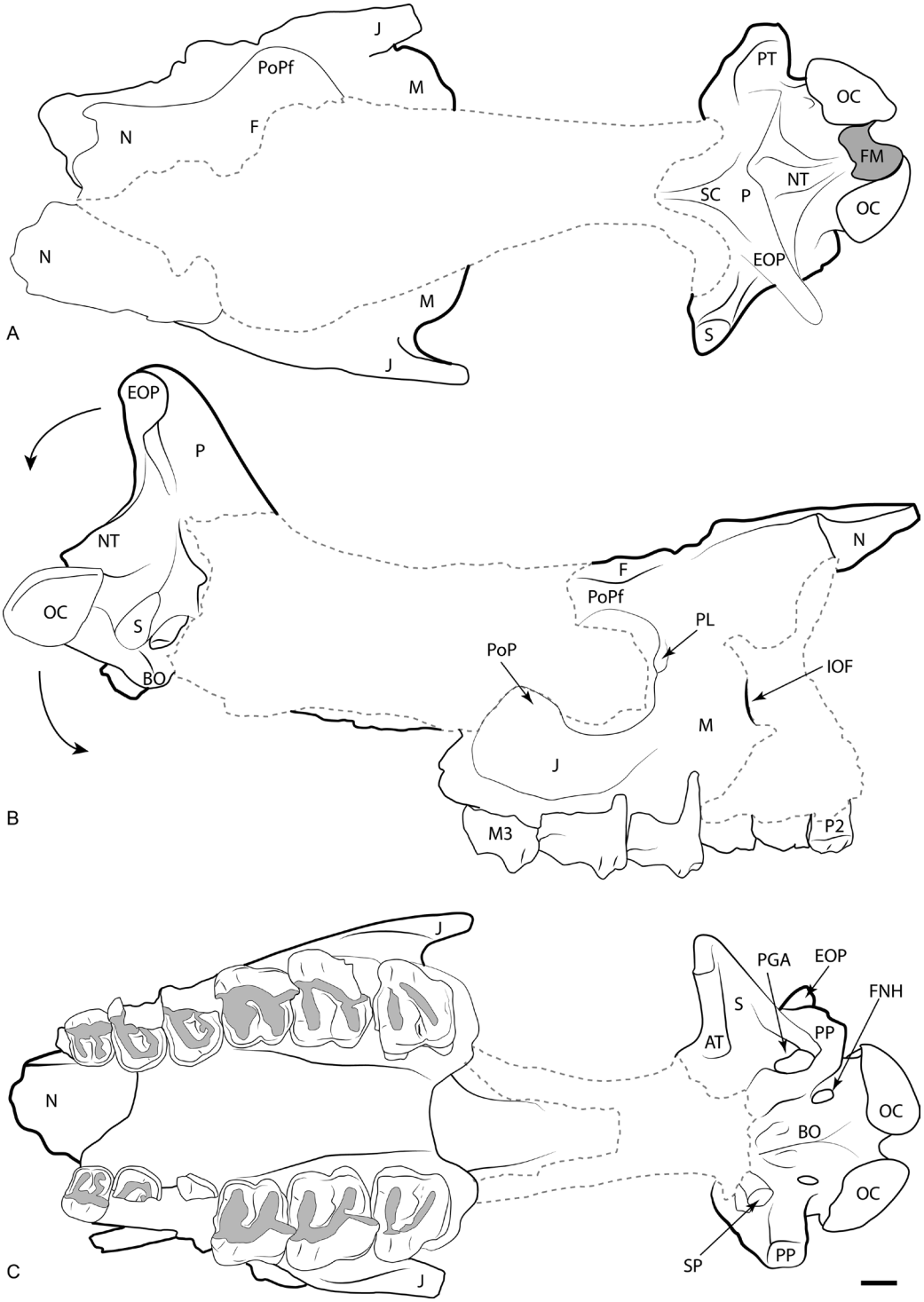

Fig. 9. *Ronzotherium elongatum* Heissig, 1969 from Pernes (early Oligocene?). Drawing of the skull FSL-9601. **A**. Dorsal view. **B**. Right lateral view. **C**. Ventral view. The arrows indicate the hypothetical position of the posterior part of the skull. Abbreviations: AT = articular tubercle; BO = basioccipital; EOP = external occipital process; F = frontal; FM = foramen magnum; FNH = foramen nervi hypoglossi; IOF = infraorbital foramen; J = jugal; M = maxilla; N = nasal; NT = nuchal tubercle; OC = occipital condyle; P = parietal; PGA = postglenoid apophysis; PL = processus lacrimalis; PoP = postorbital process; PoPf = postorbital process of the frontal; PP = paraoccipital process; PT = posttympanic; S = squamosal; SC = sagittal crest; SP = styloid process. Scale bar: 2 cm.

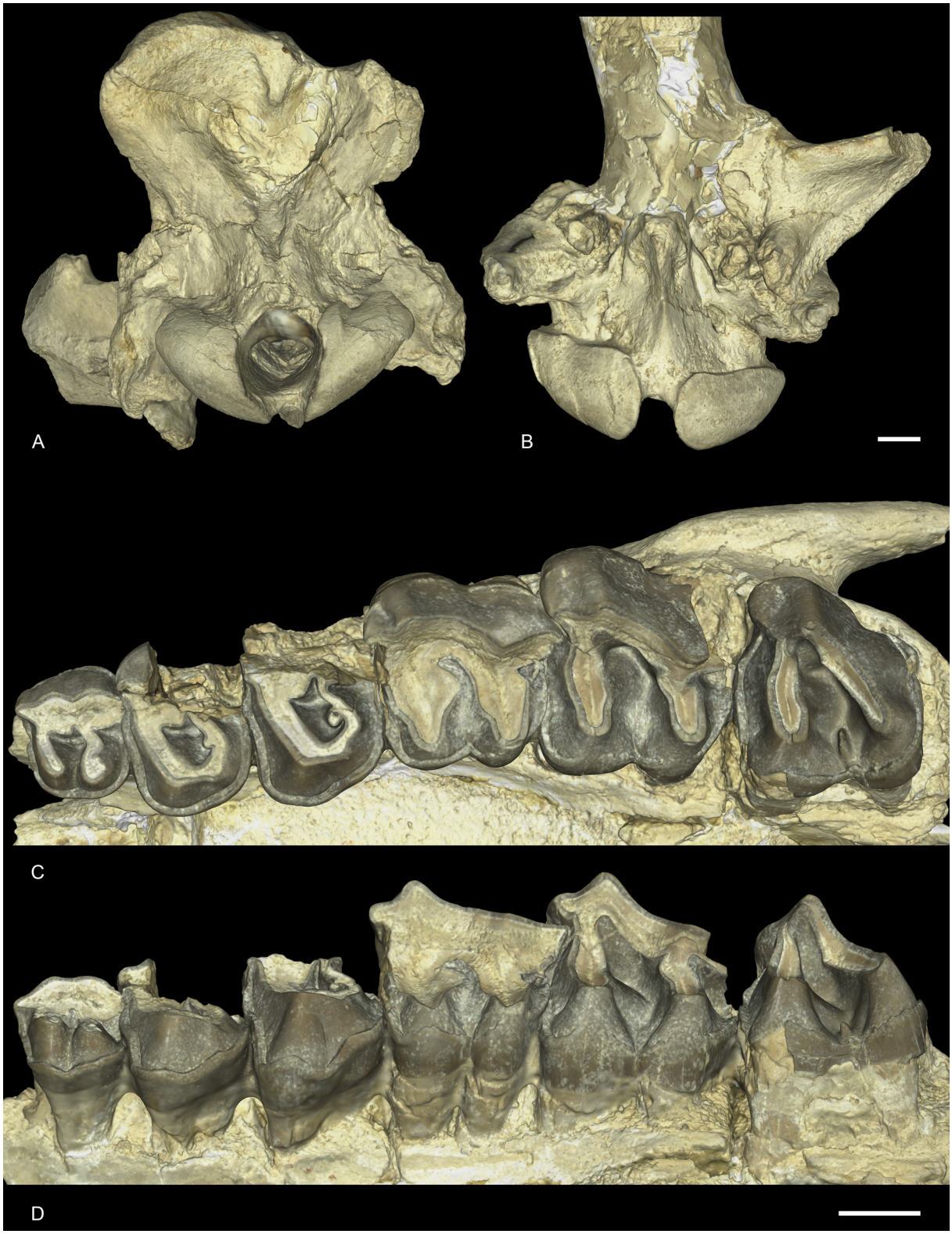

Fig. 10. *Ronzotherium elongatum* Heissig, 1969 from Pernes (early Oligocene?). – **A–B**. Skull FSL-9601. **A**. Posterior view. **B**. Close-up view of the posterior part in ventral view. – **C–D**. Left P2–M3 of the skull FSL-9601. **C**. Occlusal view. **D**. Lingual view. Scale bars: 2 cm.

The labial cingulum is strong and continuous on P2, but the ectolophs are broken on P3–4 so we cannot determine whether it was present or absent. The lingual cingulum is very strong and continuous on P2–4 and is rippled in lingual view, especially on P4. There is a short but well-defined crochet on P3–4. It is simple, directed towards the protocone and completely missing on P2. The metaloph is not constricted and the postfossette is narrow. The antecrochet is always absent. The protocone and hypocone of P2 are connected by a low bridge and are rather equal in size. The protoloph of P2 is directed slightly postero-lingually while the metaloph is S-shaped and transverse. They are both joining the ectoloph. The paracone and metacone folds of P2 are present and wide. The medifossette is always absent on premolars and the protocone is never constricted. The protocone and hypocone of P3–4 form a lingual wall, and a lingual groove is present. The metaloph of P3–4 is S-shaped and directed postero-lingually. The protoloph and metaloph of P3–4 are connected to the ectoloph.

The labial cingulum is strong under the metastyle of M1–2 and the parastyle of M1 but is absent otherwise. The lingual cingulum is also strong and almost completely continuous on all upper molars. It is only fainted under the hypocone of M1 and the protocone of M2. The anterior and posterior cingulum are continuous. The antecrochet is present, but poorly defined and only appears effectively on the protoloph with very strong wear. The crochet, crista and medifossette are always absent on upper molars. The protocone is always weakly constricted. The paracone fold is strong and there is neither a metacone fold nor a mesostyle. The metastyle and metaloph are long and the posterior part of the ectoloph is straight. The hypocone is never constricted and the anterior groove of the metaloph is very shallow or absent. The postfossette is short, but deep, below the posterior cingulum. The ectoloph and metaloph of M3 are completely fused, and the posterior groove is very shallow. It is quadrangular in occlusal view. The protoloph is transverse. There is a small crest in the median valley of the left M3, that seem to have been broken on the right one. It may be caused by individual variation and is completely absent on other molars.

Remark

This species is the most recently one erected, though it was originally considered a subspecies of *R. filholi*. Brunet (1979) and subsequent authors considered it as a junior synonym of *R. filholi*. Based on our comparative work and our phylogeny, we consider it as a valid species.

Ronzotherium filholi (Osborn, 1900)
Figs 11–14

Aceratherium filholi Osborn, 1900: 240–243, figs 7, 8a.
Badactherium latidens Croizet, 1841: 79 (nomen nudum).
Rhinoceros brivatensis Bravard, 1843: 408–410 (nomen oblitum).
Rhinoceros incisivus Blainville, 1846: pl. XII (Ongulogrades, 'Auvergne') (misidentification).
Rhinoceros minutus Thomas, 1867: 239 (misidentification).
Rhinoceros tetradactylus Filhol, 1877: 126 (misidentification).
Rhinoceros lemanensis Lydekker, 1886: 153 (from Caylux) (misidentification).
Praeaceratherium minus Koch, 1911: 377–379, 385–387 (misidentification).
Paracaenopus kochi Kretzoi, 1940: 92.
Ronzotherium filholi elongatum Heissig, 1969: 46–55, figs 16–17, 18a–c, 19 (from Villebramar) (misidentification).

Ronzotherium velaunum – Aymard 1856: 235. — Boada-Saña *et al*. 2007: 6.
Rhinoceros brivatensis – Aymard 1856: 235.
Badactherium latidens – Landesque 1888: 21, 27.

Rhinoceros latidens – Landesque 1888: 27.
Aceratherium lemanense – Pavlov 1892: 184, pl. V, fig. 7 (from Quercy).
Ronzotherium filholi – Deninger 1903: 95. — Wood 1929: 2 (= "*Praeaceratherium minus*" = *Paracenopus*). — Lavocat 1951: 116–118 (from Bournoncle). — Brunet & Guth 1968: 573–575, pl. I. — Heissig 1969: 38. — Brunet 1970: 2535; 1979: 105–152, 159–161, figs 8, 9a, c, e, 10a, 11–14, 16b, pls IX–XIV, XVIa, XIXm–n, XX–XXV. — Santafé Llopis 1978: 44. — Antoine 2002: 32. — Becker 2003: 231, pl. IIh (from Bressaucourt); 2009: 493–495, fig. 4g (from Bressaucourt).
Praeaceratherium filholi – Abel 1910: 18–20, 44–45.
Acerotherium filholi – Roman 1910: 1559 (from Quercy and Puylaurens); 1912a: 5, 27, 45, 51–53, fig. 16a (from Quercy, Villebramar and Puylaurens).
Praeaceratherium filholi – Koch 1911: 377–379, 385–386. — Wood 1927: 232/72.
Acerotherium lemanense – Roman 1912a: 60–61 (from Montans).
Aceratherium filholi– Stehlin 1914: 185 (from Bressaucourt).
Paracaenopus filholi – Breuning 1924: 7, 17–20, figs ?6, 7.
? *Aceratherium filnoli* [sic] – Crusafont Pairó 1967: 116.
Ronzotherium filholi filholi – Heissig 1969: 39–46, figs 12–15, 25c–d, 26a–b.
Ronzotherium kochi – Heissig 1969: 36–37. — Adrover *et al*. 1983: 126. — Codrea & Şuraru 1989: 322. — Guérin 1989: 4. — Uhlig 1999a: 477–479. — Codrea 2000: 38–42, fig. 8.
Epiaceratherium ? *kochi* – Brunet 1979: 158.
Allacerops kochi – Russell *et al*. 1982: 58.
"*Ronzotherium*" *kochi* – Radulescu & Samson 1989: 302.
Epiaceratherium sp. – Becker 2009 (= *Ronzotherium kochi*).

Non *Ronzotherium filholi* – Lavocat 1951: 116, pl. 19 fig. 3, pl. 26 fig. 1 (from Vendèze) (misidentification).
Non *Ronzotherium filholi* – Brunet 1979: 105, 134 (from Pernes, Kleinblauen and Bumbach) (misidentification).
Non *Ronzotherium filholi* – Becker 2003: 230–233, pl. IIa–f (from Kleinblauen and Bumbach) (misidentification).
Non *Ronzotherium filholi* – Becker 2009: 493–495, fig. 4h–l (from Kleinblauen) (misidentification).

Historical diagnosis

(From Osborn 1900): "Large upper premolars, simple, unlike molars, with incompletely formed crests; upper molars with internal cingulum and strong protoconule [= paracone] fold, small antecrochet, no crochet; depression in posterior face of metaloph of third molar; third and fourth lower premolars with depressed and incomplete posterior crests. Measurements: P2–M3=224."

However, this diagnosis could refer to several species of *Ronzotherium* since these characters are mostly synapomorphies of the genus. Therefore, we emend the diagnosis based on the type specimens from the Phosphorites du Quercy. Other emended diagnoses were provided by Heissig (1969) and Brunet (1979), but they were not only based on the type material, but also on referred material from other localities. We emend here the diagnosis based on our phylogenetic analysis.

Emended diagnosis

The coronoid process of the mandible is rather weak. The upper premolars are large, simple, non-molariform, with incompletely formed protoloph and metaloph, and labial cingulum always present; P2 molariform, protocone and hypocone usually fused on P3–4, strong, simple and continuous lingual cingulum, usually without ridges; crista sometimes present on P3; metaloph of P2–4 discontinuous; upper molars with strong and continuous lingual cingulum except under the hypocone of M1, almost no labial cingulum, small antecrochet, no crochet, and a posterior groove on the ectometaloph of M3; lower cheek teeth with strong and continuous labial cingulum and lingual cingulum in the opening of the posterior valley; d/p1 usually present and two-rooted, the paraconid of p2 is developed; the magnum facet of the McII is straight; high proximal articulation of the fibula with the tibia; the expansion of the calcaneus facet is wide and low on the astragalus; proximal border of the anterior side of the MtIII straight and intermediate reliefs of the metapodials low and smooth.

It differs from *R. velaunum* by the deep median constriction of the distal humeral articulation and from *R. elongatum* by its close frontoparietal crests, its straight occipital crest and its poorly developed processus posttympanicus and its constricted metaloph on P3–4 (hypocone not connected to the ectoloph).

It further differs from *R. elongatum* and *R. romani* by its sharp angle at the anterior tip of the zygomatic process and the higher posterior side of the scaphoid compared to its anterior side.

Type material

Holotype

FRANCE • maxilla fragment with right and left cheek teeth rows with P2–M3; Quercy Phosphorites (southwestern France); MNHN.F.QU7232.

Paratypes

FRANCE • 1 left mandible fragment; Quercy; MNHN.F.QU7202 • 1 right mandible fragment; Quercy; MNHN.F.QU7201.

Osborn (1900) designated a left mandible fragment (MNHN.F.QU7202) also from Quercy as "cotype", which was followed by Heissig (1969), who also added its right counterpart (MNHN.F.QU7201) from the same individual. These two hemimandibles should be regarded as paratypes. The upper and lower anterior dentition are unknown.

Additional material

Old collections from Quercy are preserved in almost every large European institution, including, but not limited to the MNHN, TLM or NMB, but are problematic because the exact age and locality are unknown. The specimens examined from these collections that we mention in the text are:

FRANCE – **Quercy** • 1 right maxillary fragment with P1-2; MNHN.F.QU16445 • 1 left hemimandible with m1-3; MNHN.F.QU17193 • 1 right scaphoid; NMB-QV-275 • 1 right lunate; NMB-QE-440 • 1 left pyramidal; NMB-QE-433 • 1 left magnum; NMB-QE-472 • 1 left cuboid; NMB-QE-362. – **Bournoncle-Saint-Pierre** • 1 astragalus; MNHN.LIM7.

ROMANIA – **Cluj-Napoca** • 1 right maxilla with P2–M3; MBT 1509.

GERMANY – **Espenhain** • 1 left radius; BSPG-2008-I-44. – **Möhren 4** • 1 left D4; BSPG-1966-XXXIII-47 •1 left MtIV; BSPG-1971-V. – **Möhren 7** • 1 left P1; BSPG-1969-XXIV-151 • 1 left P3; BSPG-1969-XXIV-150 •1 right p3/4; BSPG-1969-XXIV-71 • 1 fragment of left lower molar; BSPG-1969-XXIV-152 • 1 right distal ulna; BSPG-1969-XXIV • 1 right proximal McIII; BSPG-1969-XXIV • 1 fragmentary astragalus; BSPG-1969-XXIV-183 • 1 right MtII; BSPG-1969-XXIV-73 • 1 left MtIII; BSPG-1969-XXIV-156. – **Möhren 11** • 1 right calcaneum; BSPG-1971-V-11.

Type horizon and locality

Unknown horizon and locality in the Phosphorites du Quercy.

Stratigraphical distribution

Possibly restricted to the early Oligocene.

Geographical distribution

France: Phosphorites du Quercy, Bournoncle Saint-Pierre, Villebramar, Penchenat (= Moulinet?), Puylaurens. Germany: Möhren 4, 7/16, 19, 20, Burgmagerbein 8, Ronheim 1, Grafenmühle 6. Romania: Cluj-Napoca. Spain: Montalbán. Switzerland: Bressaucourt.